Available online at sjuoz.uoz.edu.krd

Science Journal of University of Zakho

Vol. 12, No. 1, pp. 22 – 33 January-March, 2024

journals.uoz.edu.krd

p-ISSN: 2663-628X
e-ISSN: 2663-6298

INVESTIGATION OF THE IMPACT OF DIFFERENT PARAMETERS ON THE MORPHOLOGY OF ELECTROSPUN POLYURETHANE NANOFIBERS

Fatima Taher Sabri [a]*, Manaf Ali Mahammed [b]

[a] Department of Physics, College of Science, University of Duhok. (nimazaxo@gmail.com)

[b] Scientific Research Center, College of Science, University of Duhok. (manaf.zivingy@uod.ac)

Received: 10 Sep., 2023 / Accepted: 14 Nov., 2023 / Published: 16 Jan., 2024. https://doi.org/10.25271/sjuoz.2024.12.1.1203.

ABSTRACT:

In this research, nonwoven nanofiber mats were prepared using the electrospinning method for the solution of polyurethane polymer dissolved in acetic acid. Effects of solution concentration, solution flow rate, as well as high voltage on the morphonology and wettability of the prepared nanofibers were studied. Nanofiber morphology was investigated through the analysis of scanning electron microscopy (SEM) micrographs using ImageJ software, while the wettability of the nanofiber mat surfaces was studied through the measurement of the contact angle. Results revealed that when the concentration of the solution was changed from 8wt% to 12wt%, the average nanofiber diameter showed a significant increase from 0.326 µm to 0.380 µm, while the contact angle increased from 39 degrees to 79 degrees. Results also showed that when the applied high voltage was changed from 10 KV to 25 KV, the average nanofiber diameter decreased and then increased within the range of 0.380 to 0.497 µm and that the contact angle was increased from 81 degrees to 108 degrees showing an obvious switching from hydrophilic towards hydrophobic surface. When the syringe pump flow rate was changed from 0.012 ml/min to 0.02 ml/min, morphology measurements showed that the average nanofiber diameter showed a significant increase from 0.351 µm to 0.456 µm, and the surface contact angle was also increased from 43 degrees to 98 degrees. Finally, the results of Fourier Transform Infrared Spectroscopy (FTIR) and X-ray diffraction analysis (XRD) tests showed that the electrospun polyurethane polymer material used in this work was not changed during the electrospinning process.

KEYWORDS: Electrospinning, Nanofibers, Polyurethane, Concentration, Flowrate, High voltage.

1. INTRODUCTION

Polyurethane (PU) is a versatile polymer that contains a urethane group (–NH–(C=O)–O–) in common. PUs are typically formed through the polyaddition polymerization reaction between polyisocyanates and polyols. Desired properties can be customized by selecting the type of isocyanate and polyols or combinations thereof. By altering the structure of PUs, their properties can vary over a wide range. The ability to adjust the structure during processing is one of the key advantages of PUs over other types of polymers. PU is often preferred as a material for constructing nanoweb structures due to its chemical stability, mass transport properties, strong mechanical characteristics, and excellent nanofiber-forming attributes (Hale Karakaş *et al*., 2018; Akduman & Kumbasar *et al*., 2017; Panwiriyarat *et al*., 2013).

Nanofibers are extremely thin fibers with nanometer dimensions ranging from a few to 1000nm. Their superior properties, such as a high surface area-to-volume ratio, small pore diameters, high porosity, low density, and superior mechanical properties, make them ideal candidates for a wide variety of applications (Williams *et al*., 2018; Colmenares-Roldán *et al*., 2017; Ungur & Hrůza *et al*., 2017; Nitanan *et al*., 2012; Barhoum *et al*., 2019). Various methods can be employed for the production of nanofibers, including template synthesis, drawing, self-assembly, electrospinning, and phase separation (Eatemadi *et al*., 2016; Sharma *et al*., 2015; Beachley & Wen *et al*., 2010).

However, electrospinning stands out as a particularly promising technique due to its numerous advantages, such as versatility, ease of use, flexibility, cost-effectiveness, and the ability to produce nanofibers with small dimensions (Emad Abdoluosefi & Honarasa *et al*., 2017). Electrospinning is a fantastic method for producing nanofibers. To initiate the process, a polymer solution is loaded into a syringe coupled to a spinneret. When a strong electric field is supplied to a solution, it charges up, resulting in electrostatic forces. These forces cause a droplet to develop at the spinneret's tip. As the electric field becomes stronger, the droplet changes into a conical shape known as the Taylor cone, finally creating a thin jet of the polymer solution. As it moves toward the collector, the jet lengthens, and the fast evaporation of the solvent hardens the polymer into ultrafine fibers (H Karakaş et al., 2013; Williams *et al*., 2018).

During the electrospinning procedure, the morphology and uniformity of nanofibers are influenced by several parameters, which can be divided into three major groups: (a) parameters of the polymer solution, (b) parameters of the setup, and (c) environmental conditions. The parameters of a polymer solution include the molecular weight, viscosity, surface tension, and conductivity of the solution. The setup parameters include the high applied voltage, solution flow rate, needle diameter, and tip-to-collector distance. Humidity and temperature make up the ambient conditions (Sorlier, 2007; Bhardwaj & Kundu *et al*., 2010). By selecting the appropriate molecular and process parameters, nearly all polymers can be transformed into nanofibers via electrospinning.

Electrospun polyurethane nanofiber mats with strong mechanical properties have a multitude of potential applications in high-performance air purifiers, protective textiles, wound dressing materials, sensors, biomedical applications, drug delivery, etc. (Akduman & Kumbasar *et al*., 2017).

Several studies have investigated the production of polyurethane (PU) nanofibers through electrospinning. For instance, Karakaş *et al*., (2018), Demir *et al*. (2002), Yang *et al*. (2010), B. Li *et al*. (2020), Firoozi *et al*. (2016), Kiliç *et al*. (2018), Choi *et al*. (2014), Emad Abdoluosefi and Honarasa. (2017), Hu *et al*. (2021), Öteyaka *et al*. (2022), Banuškevičiute *et al*. (2011), Zhuo *et al*. (2008), and Rabbi *et al*. (2012) have given significant

* Corresponding author

information on influential factors impacting nanofiber morphology and underlined the necessity of carefully regulating parameters in the electrospinning process to generate uniform PU nanofibers without beads and desirable nanofiber diameters. Briefly, the idea that solution concentration as being the most important parameter among these parameters is well supported in the literature. Larger fiber diameters often result from greater concentration and flow rates, while smaller fiber diameters typically come from longer nozzle-collector lengths and higher electric potentials. Understanding and controlling these parameters are essential for tailoring the characteristics of nanofibers in the electrospinning process.

The purpose of this study was to investigate Electrospun polyurethane nanofibers comprehensively, with a particular focus on the effects of PU concentration, applied high voltage, and flow rate on fiber morphology. Four various PU concentrations (8%, 9%, 10%, and 12%), voltages spanning from 10 to 25 kV, and five distinct flow rates (0.012, 0.014, 0.016, 0.018, and 0.020 ml/min) were investigated in details to determine how these variables affect the resulting fiber diameter and surface morphology.

2. MATERIALS AND METHODS

2.1 Materials

The polyurethane material used in this study was sourced from Sigma-Aldrich's Selectophore™ product line, designated as 'Quality Level 200' with an ion-selective grade. It was supplied in bead form, chosen for its high purity (99.5%), a molecular weight of 100,000 g/mol, and a relative density of 1.140 g/cm³. Acetic acid (CH3COOH), an essential component, was obtained and used as the solvent. The nanofibers in this research were meticulously produced using a sophisticated electrospinning set-up. This state-of-the-art machine, as illustrated in Figure 1, incorporates a high-voltage power supply (0-40 KV purchased from Baoding Chuang Rui Precision Pump Co., Ltd./China), precise needle-to-collector distance adjustment, a digital control syringe pump (ZS 100), and a grounded collector which was covered with a piece of thick aluminum (Al) sheet. ensuring optimal performance and reproducibility of the nanofiber production process.

2.2 METHODS

2.2.1 Electrospinning Process:

The electrospinning system consists of three main components: a syringe pump for pumping the polymer solution through the needle, a high-voltage power supply used to create a high electric potential difference between the spinneret (the tip of the syringe needle), and a collector, which is a conductive plate or drum serving as the target for collecting the electrospun fibers. The loaded syringe is connected to the syringe pump. The high-voltage power supply is then activated, creating a strong electric field between the spinneret (the needle's tip) and the collector. The positive electrode is connected to the needle tip, and the negative electrode is linked to the collector.

The distance between the needle tip and the collector is finely adjusted to control the behavior of the polymer jet during electrospinning. Under the influence of the electric field, the charges within the polymer solution leads to the formation of a characteristic conical droplet at the apex of the spinneret, known as the 'Taylor cone.' As the electric field intensifies, the repulsive forces overcome the surface tension of the solution, causing the Taylor cone to release a continuous stream of polymer solution as this jet progresses toward the collector, rapid solvent evaporation leads to the formation of nanofibers. These nanofibers are guided by the electric field and drawn toward the collector, where they are deposited, forming a nonwoven mat in either a random or aligned pattern, depending on the collector's design (Z. Li *et al*., 2016; Gao *et al*., 2021; Baji *et al*., 2010).

2.2.2 Preparation of Polyurethane solution:

In the solution preparation phase, PU pellets were precisely weighed, as illustrated in Figure 2. These pellets were then dissolved in acetic acid at varying concentrations (8%, 9%, 10%, and 12wt%) under continuous stirring using a magnetic stirrer. The stirring process was maintained for an uninterrupted 48-hour period at room temperature to ensure the complete dissolution of the polymer. To provide more specific details regarding the formulations, the 8% solution was created by combining 0.32g of PU polymer with 4 mL of acetic acid solvent. Likewise, the 9%, 10%, and 12% solutions were prepared using 0.36g, 0.4g, and 0.48g of PU polymer, respectively, all dissolved in 4 mL of acetic acid. Subsequently, all these solutions were stored under carefully controlled environmental conditions. It is worth noting that these solutions were prepared one day before initiating the electrospinning process. A syringe with a 24G inner needle diameter was used to inject the polyurethane/acetic acid solution. The needle-to-collector distance was set at 15 cm, and the polyurethane solution was fed at rates of (0.012, 0.014, 0.016, 0.018, and 0.020) ml/min. The high-voltage power supply's positive electrode was attached to the metallic needle of the syringe that had been connected to the syringe pump, while its negative electrode was linked to the aluminum foil that covers the collector. The voltage settings were (5, 10, 15, 20, 25) kV. The high-voltage power source was then activated, and an electric field was applied between the needle and the collector. The electrospinning operation was conducted at room temperature.

After electrospinning was completed, the nanofibrous web was meticulously removed from the Al foil and stored for further examination. Using ImageJ and Origin Software Lab, the average fiber diameters of the obtained nanofibers' SEM images were measured. For every experimental condition, at least 100 unique fibers were measured.

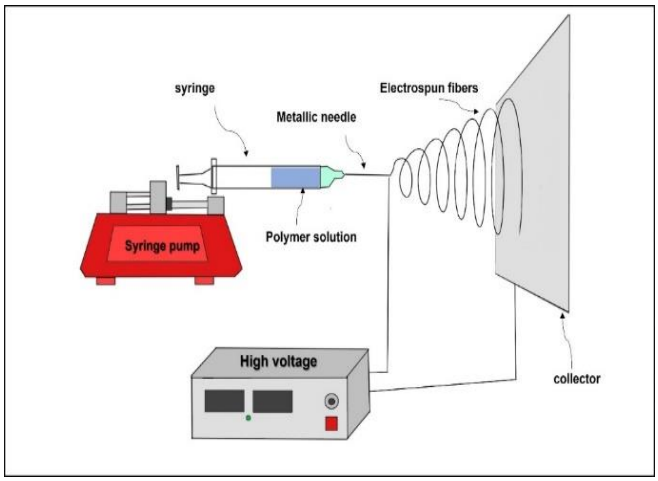

Figure1: Basic set-up of electrospinning.

2.2.3 Characterization

The samples underwent morphological analysis using scanning electron microscopy (SEM). For precise quantification of nanofiber diameter, the ImageJ analysis software and Origin Lab software were employed. In each experimental scenario, over 100 distinct fibers were measured. Subsequently, a histogram was constructed using the gathered data from each sample to illustrate the distribution of fiber dimensions and determine their mean diameter. Exploration of the chemical composition of the polyurethane nanofibers was conducted via Fourier-transform infrared spectroscopy (FTIR, Shimadzu 1800, Japan). This method yielded precise insights into the molecular

bonds and functional groups present within the nanofibers. Complementary X-ray diffraction (XRD) analysis was employed to unveil the crystallographic attributes of the nanofibers, offering a deeper understanding of their structural characteristics. Furthermore, energy-dispersive X-ray spectroscopy (EDX) was applied to perform elemental analysis on the nanofibers. Additionally, an assessment of the Electrospun mesh's wettability was carried out by measuring the contact angle of water. The sessile drop technique, coupled with ImageJ software (version 1.53a), was used to evaluate the contact angles of de-ionized water droplets (~2µL). This measurement facilitated the determination of surface properties and hydrophilicity of the nanofiber material.

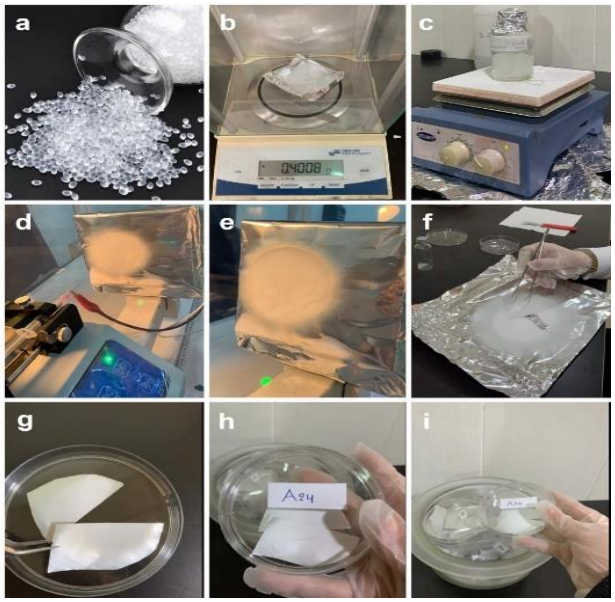

Figure 2: steps of nanofiber production.

3. RESULTS AND DISCUSSION

In this study, the impact of polyurethane (PU) solution concentration, flow rate, and high voltage on the morphology and wettability of Electrospun polyurethane nanofibers was investigated. The obtained results will be introduced and discussed throughout the following paragraphs.

3.1 Effect of concentration:

Figure 3 presents Scanning Electron Microscopy (SEM) images and the corresponding size distribution analysis of Electrospun polyurethane nanofibers. These nanofibers were fabricated using distinct concentrations (8%, 9%, 10%, and 12%) of the polymer solution. Throughout the experimental process, all other material and process parameters remained constant. The electrospinning process was performed under these conditions, including a high voltage of 15kv, a tip-to-collector distance of 15cm, and a flow rate of 0.016 ml/min. The results emphasize the substantial impact of polymer solution concentration on the nanofibers' size and morphology.

Figure 3(a) depicts nanofibers produced at an 8wt% concentration, SEM image shows a non-uniform morphology with the presence of large-sized particles and beads. This indicates that the concentration was inadequate, resulting in poor viscosity and the inability to create continuous nanofibers and uniform morphology. This was consistent with a prior work by Karakaş *et al*., (2018), who also found beads at low polyurethane concentration owing to inadequate stretching of the charged jet. In contrast, B. Li *et al.* (2020) effectively manufactured nanofibers with a smooth and homogenous web at the same concentration. However, it is worth mentioning that the diameter of the produced nanofibers at this concentration throughout this work was 0.326µm.

Figures 3(b) and 3(c) show SEM images of nanofibers that were produced at concentrations of 9wt% and 10wt%, respectively. The findings show that beads are still present along the nanofibers (beads-on-string structures) in both samples with a reduction in the bead size observed at the 10wt% concentration. Quantitatively, these concentrations' nanofiber diameters were 0.263µm. and 0.334µm respectively. All of these results indicate that bead formation is not eliminated by increasing the polymer concentration to 9% or 10%. To successfully prevent the development of beads, this suggests a pressing need for using an even greater concentration of polyurethane. Zuo *et al.* (2005) suggest that the presence of beads during electrospinning is associated with the instability observed in the jet of the solution. In simpler terms, when a polymeric solution is Electrospun, the flow of the liquid can become unstable, resulting in the formation of beads along the fibers. According to Fong *et al*. (1999), the breakup of the polymeric solution during electrospinning can be attributed to the influence of surface tension, which leads to the formation of beads and droplets with fibers in between. The droplets form because surface tension drives the liquid to minimize its surface area per unit mass.

Figure 3(d) displays the impact of increasing the solution concentration to 12%. Notably, a uniform morphology with no beads was observed in this case. Furthermore, the nanofiber diameter increased to 0.380 µm. These results indicate that nanofiber diameter increases with higher solution concentration and prevents bead formation. However, an unexpected decrease in nanofiber diameter was observed at a 9wt% concentration, as depicted in Figure 4. This unusual behavior might be attributed to the interplay of various factors, including solution viscosity and polymer chain entanglement. It is worth noting that these findings align with previous studies conducted by Firoozi *et al*. (2016), Kiliç *et al*. (2018) and Karakaş *et al*. (2018) who also reported an increase in nanofiber diameter with higher concentration. We found that this concentration eliminates bead formation and provides an increased diameter for the nanofibers. Considering the obtained results, the 12% concentration seems to be the optimal choice for further investigations on the effects of flow rate and high voltage.

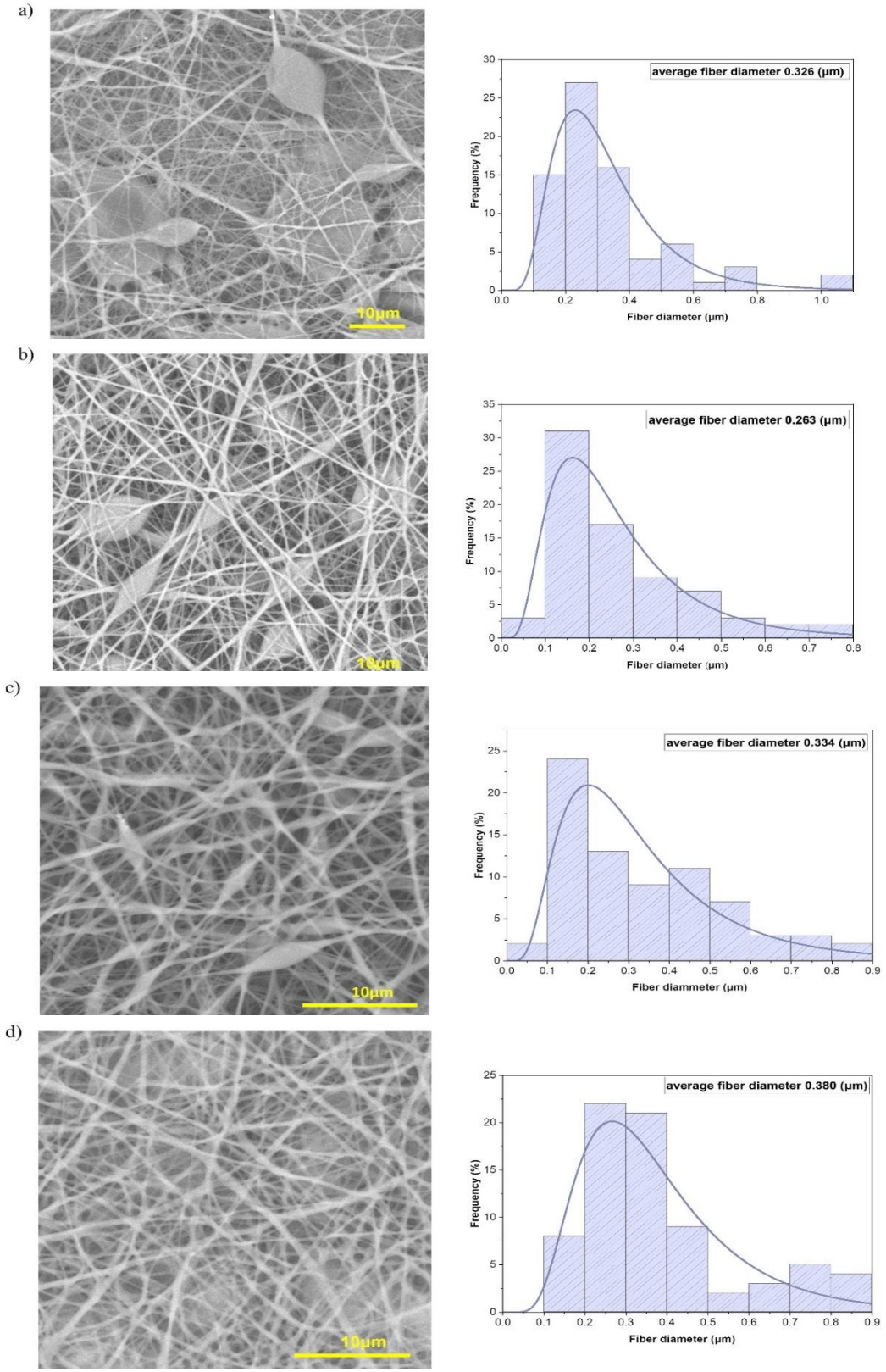

Figure 3: Scanning electron microscopy (SEM) images and fiber diameter distribution of nanofibers with different concentrations.

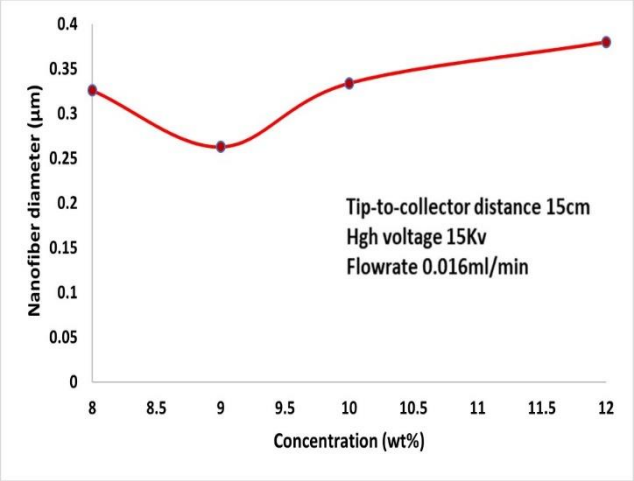

Figure 4: Effect of solution concentration on the diameter of Electro spun polyurethane nanofiber.

3.2 Effect of high voltage:

A series of five different voltage values (5, 10, 15, 20, and 25 kV) were systematically applied to the polyurethane (PU) solution to comprehensively evaluate the effect of voltage on polyurethane nanofiber diameter. A thorough knowledge of the connection between voltage and nanofiber production was the goal of this part of the experimental design. Other variables were kept constant to ensure uniformity throughout the trial, a 12wt% PU solution was used with a tip-to-collector distance of 15 cm and a feed rate of 0.016 mL/min. To allow a detailed comparison of voltage effects on the electrospinning process, these particular parameters were chosen.

At the lowest voltage of 5 kV, the electrospinning process yielded only droplets originating from the syringe, with no successful formation of nanofibers. As a result, no fibers were able to be collected on the designated collector. This outcome suggests that the applied voltage was insufficient to generate the necessary electric field for the electrospinning process, leading to the lack of fiber formation. It is important to note that electrospinning relies on the electrostatic attraction between the polymer solution and the collector, a process facilitates by a high voltage.

(a) 8wt%, (b) 9wt%, (c) 10wt%, and (d) 12wt%. The SEM images are magnified at 2500x, 5000x, 5000x, and 5000x, respectively.

Figure 5 presents SEM images and the size distribution of nanofibers at high voltages of 10 kV, 15 kV, 20 kV, and 25 kV. Notably, as we increased the electric field strength, we observed the formation of nanofibers with a smooth and uniform morphology. Their diameters exhibited a slight decrease from 0.426µm to 0.380µm at 10 kV and 15 kV. However, at 20 kV and 25KV, there was an increase to 0.474µm and 0.497µm respectively. This demonstrates that when the voltage was raised, the resulting nanofibers generally became thicker, with the exception of a decrease at 15 kV, as depicted in Figure 6. These findings line up with the study done by Emad Abdoluosefi & Honarasa *et al*., (2017), who examined the impact of voltage on Electrospun TPU nanofibers. They used various voltages between 10 and 30 kV while keeping the TPU concentration at 12 weight percent and the flow rate at 1 mL/h. According to their findings, the nanofiber diameter reduced at 10 kV and 20 kV before increasing once again at 30 kV.

This emphasizes the intricate relationship between voltage and nanofiber morphology. Our experimental results also closely match the trend observed in another study by Matabola *et al*. (2011) who also noticed a non-monotonic pattern in the average nanofiber diameter concerning voltage. Specifically, there was an initial decrease in nanofiber diameter, followed by an increase and another subsequent decrease. Chen & Lin *et al*. (2020) revealed a diminishing trend in nanofiber diameter at voltage levels of 15, 20, and 25 kV, succeeded by a subsequent augmentation observed at 30 KV. However, Choi *et al*. (2014) and Demir *et al*. (2002) depicted that the average diameter of the produced nanofibers increased by increasing the applied voltage. In their work, Choi *et al* (2014) utilized a PU/DMF solution to investigate the effect of an electric field on fiber morphology. They conducted the analysis using a fixed polymer concentration of 10% and a collector distance of 7 cm. The electric field varied from 5 to 20 kV. To collect the fibers, they maintained a rotation speed of 90 rpm on a collection drum covered with a stainless-steel film. Additionally, the experiments were conducted in a chamber with relative humidity below 50%. Figure (6) shows the effect of high voltage on the diameter of Electrospun polyurethane nanofiber.

a)

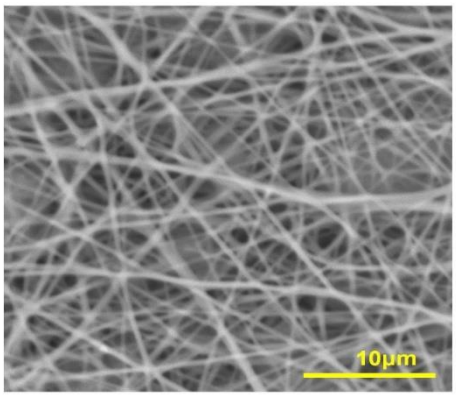

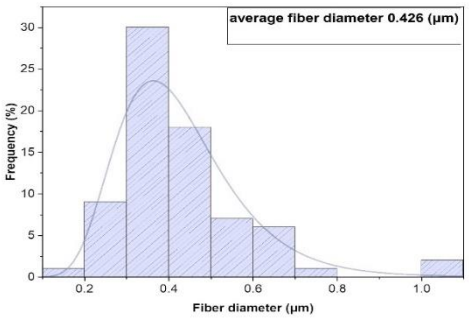

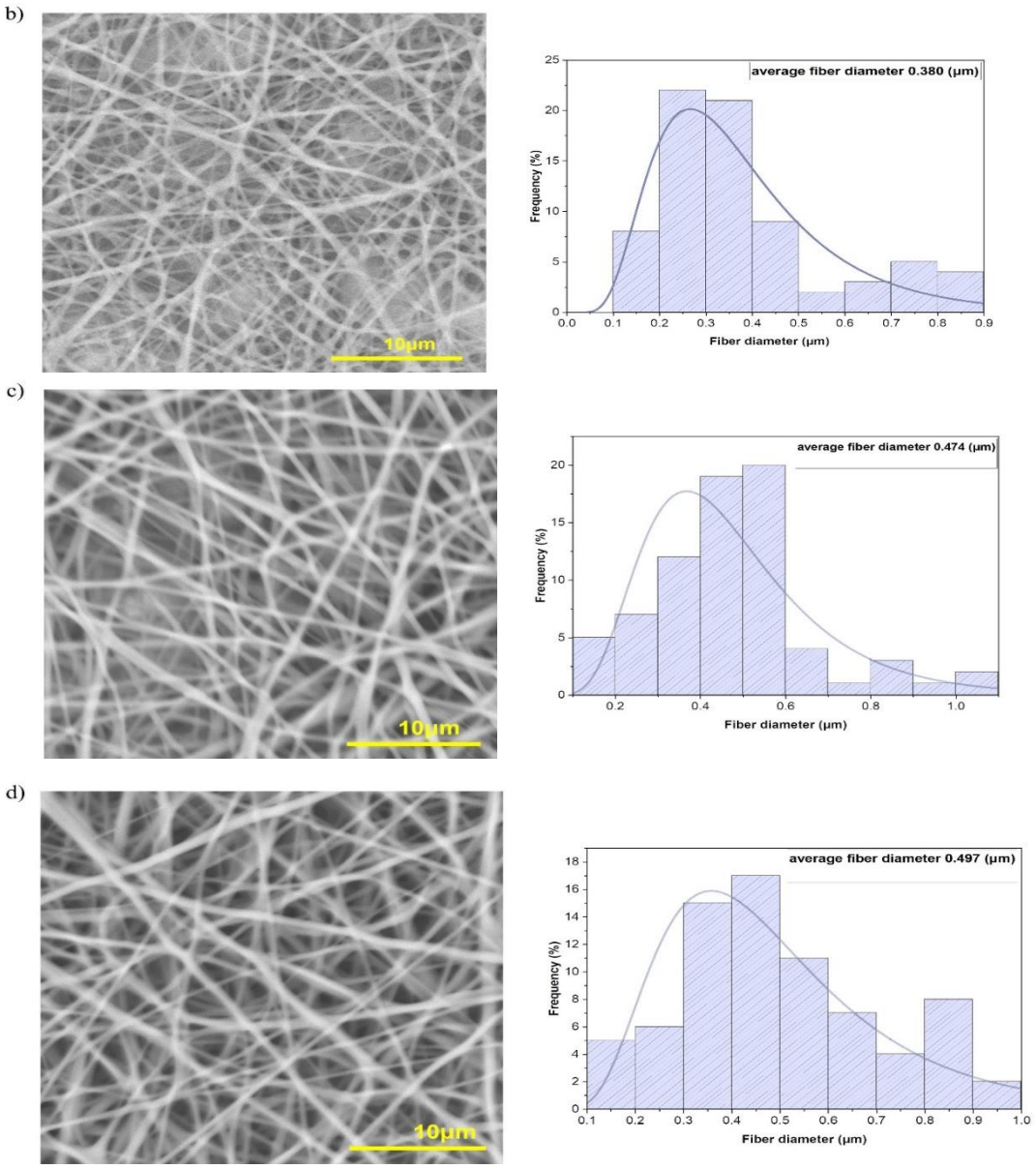

Figure 5 SEM images of Electrospun polyurethane nanofibers at a concentration of 12wt% and a flow rate of 0.016 ml/min, showcasing the influence of applied voltage: (a) 10kV, (b) 15kV, (c) 20 kV, and (d) 25 kV. All images were captured at a magnification OF 5000x.

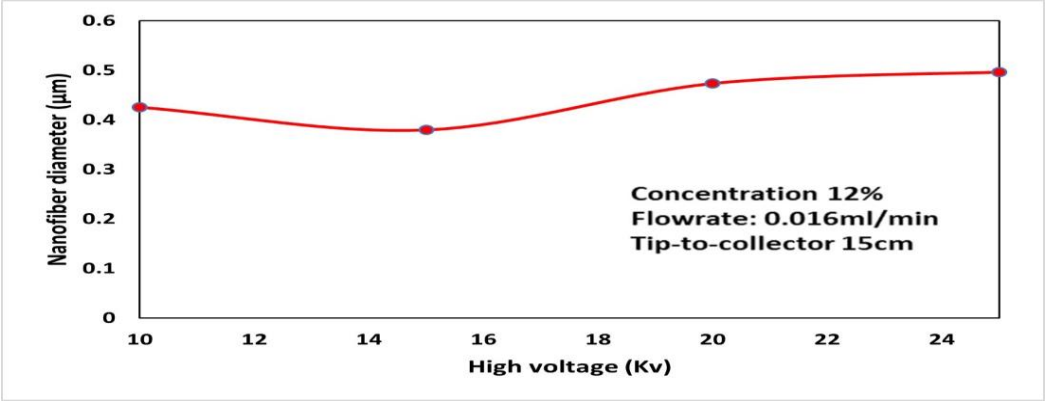

Figure 6: Effect of voltage on the diameter of Electrospun polyurethane nanofiber.

3.3 Effect of flow rate:

Five different flow rates (0.012, 0.014, 0.016, 0.018, and 0.020 ml/min) were studied to determine the effect of flow rate on the diameter of polyurethane nanofibers after investigating the effects of voltage and concentration while maintaining other parameters constant. Figure 7 displays the findings from the study of the nanofiber size distribution and the scanning electron microscopy (SEM) pictures.

According to the SEM results in Figure 7, the nanofiber diameter exhibits a modest increase as the flow rate increases. Specifically, the nanofiber diameters measured were 0.351 µm, 0.362 µm, 0.380 µm, 0.404 µm, and 0.457 µm at flow rates of 0.012 ml/min, 0.014 ml/min, 0.016 ml/min, 0.018 ml/min, and 0.020 ml/min, respectively. These findings indicate a linear relationship between flow rate and nanofiber diameter, as illustrated in Figure 8. These results are consistent with a prior study by Kiliç *et al*., (2018) where they also observed that increasing the flow rate led to an increase in nanofiber diameter. Because higher flow rates cause a greater volume of polymer to be ejected from the spinneret in a given amount of time and let to incomplete stretching, which in turn encourages the development of thicker fibers. In spite of this, it is very necessary to keep the flow rate modest in order to provide the solvent with an adequate amount of time to evaporate. The vaporization procedure is vital because it helps the nanofibers to become more solid and so prevents the production of undesired beads. It is now feasible, via the optimization of the flow rate, to manufacture nanofibers with the diameter that is needed (Bhardwaj & Kundu *et al*., 2010; Hale Karakaş *et al*., 2012). In another investigation done by Firoozi *et al*. (2016), the flow rate had no significant influence on the size of the nanofibers, indicating that there was no significant association between the two factors.

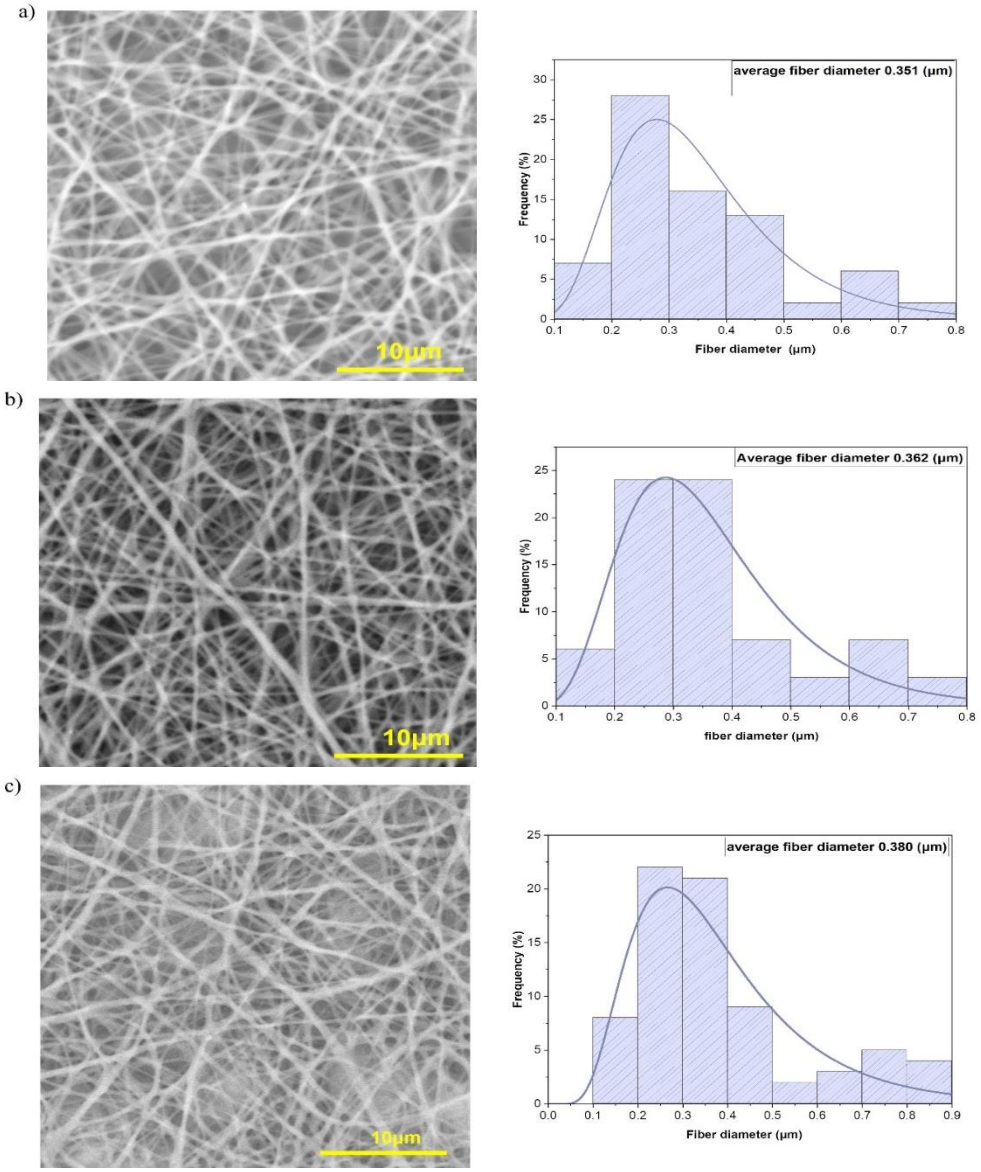

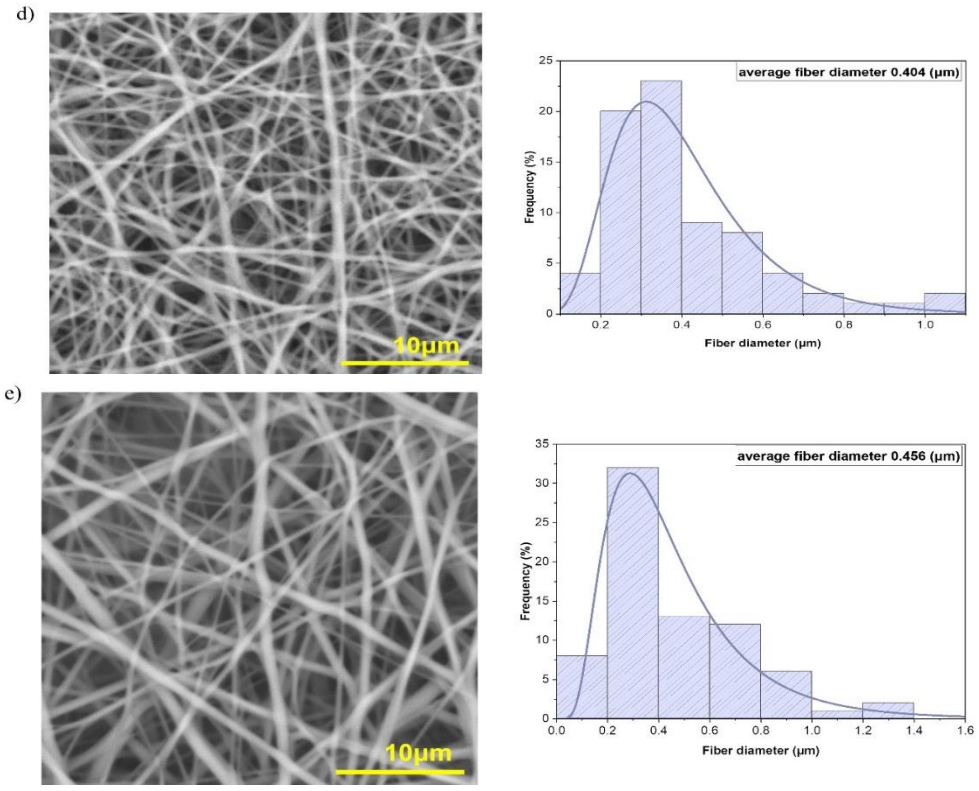

Figure7:scanning electron microscope (SEM) images of Electrospun PU nanofibers and fiber diameter distribution at a concentration of 12wt% and an applied voltage of 15 kV with different flow rates: (a) 0.012 ml/min, (b) 0.014 ml/min, (c) 0.016 ml/min, (d) 0.018 ml/min, and (e) 0.020 ml/min.

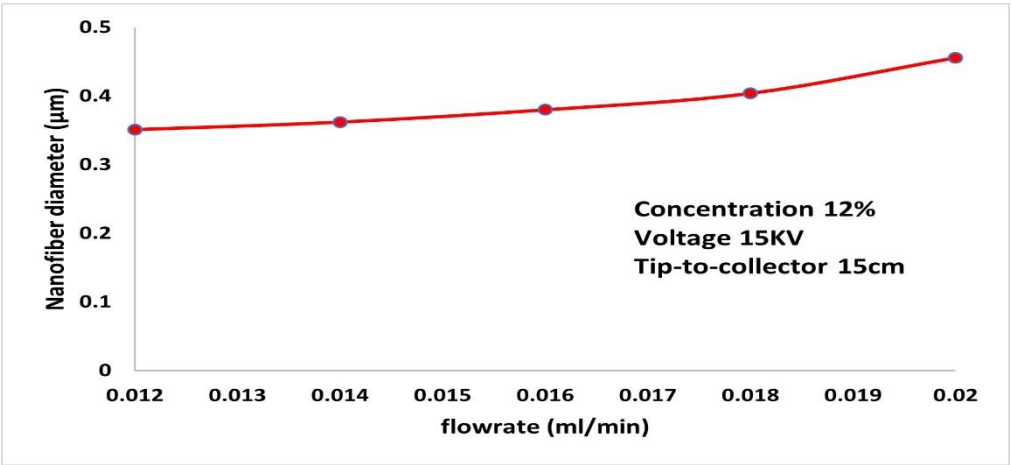

Figure 8: Effect of solution flow rate on the diameter of electrospun polyurethane (PU) nanofibers.

3.4 Wettability of PU Electrospun mat:

In order to test the wettability of the prepared polyurethane nanofiber mat, a local laboratory system was used to measure the contact angle of water droplets on the mat surface. In this investigation, a 2 µL of DI water was employed to determine the contact angle of polyurethane nanofiber mats of different parameters. as shown in Figures 9-11. Each time the droplet was pictured with a suitable digital microscope camera, the contact angle was analyzed using image-j software. As illustrated in Figure 10, and at the lowest concentration 8%, we observed a contact angle of 39 degrees. This finding indicates that the water droplet spread easily across the surface, signifying a high level of wettability and hydrophilicity.

The nanofiber mat at this concentration displayed a strong attraction to water, facilitating effective wetting of the surface. As the concentration increased to 9% and 10%, notable changes were observed in the contact angles. At 9%, the contact angle measured 53 deg, and at 10%, it increased slightly to 60 deg. These observations indicate a decrease in wettability compared to the 8% concentration, although the surface still maintained its hydrophilic characteristics. The most intriguing change was noted at the 12% concentration, where the contact angle increased significantly to 79 degrees. This observation represents a distinct departure from the hydrophilic behavior observed at lower concentrations. At 12%, the nanofiber mat exhibited a considerably reduced affinity for water, resulting in a surface that was less prone to wetting and featured a higher contact angle. This phenomenon aligns with prior researches by Khan *et al*. (2015), Yi *et al*. (2019) and Wang *et al*. (2013), where an increase in contact angle with rising concentration was also reported.

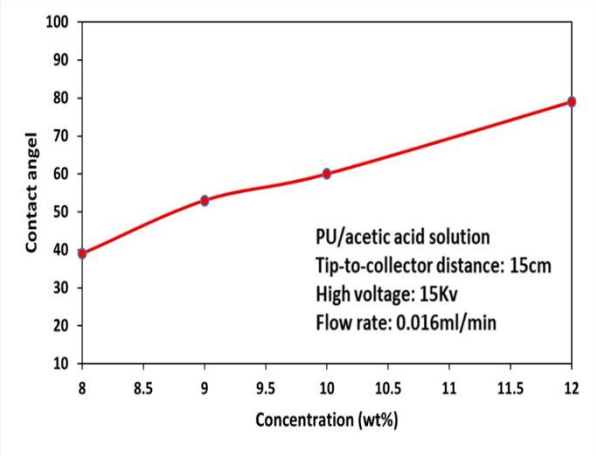

Figure 9: Variation of the contact angle of water droplet on electro spun polyurethane nanofiber mat with the solution concentration.

The contact angle measurements of PU/acetic acid nanofibers at various voltage levels are presented in Figure 11, providing valuable insights into the relationship between voltage and wettability. At 10kV, the contact angle is relatively high at 81 degrees, indicating limited wettability. However, with an increase in voltage to 15kV, there is a slight reduction in the contact angle to 79 degrees, suggesting improved wetting. The significant change occurs at 20kV, where the contact angle sharply increases to 105 degrees, signifying that at this voltage, the nanofiber surface becomes more hydrophobic and notably less wettable, at the highest tested voltage, 25kV, the contact angle remains relatively high at 108 degrees, indicating that further voltage increments do not enhance wetting.

Also as illustrated in Figure 12, we investigated how nanofiber mats interact with water at varying flow rates. The nanofiber surface displayed hydrophilic behavior with a contact angle of 43 degrees at the lowest flow rate (0.012 ml/min), promoting liquid spreading. The contact angle climbed to 74 degrees when the flow rate increased marginally to (0.014 ml/min), signaling a transition towards reduced wetting. As the flow rate was increased to 0.016 ml/min the contact angle increased to 79 degrees. This showed that the droplet found it difficult to spread and preferred to adhere to the surface. However, at 0.018 ml/min, the contact angle reached 84 degrees, showcasing stronger non-wetting. At the highest flow rate (0.020 ml/min), the contact angle significantly escalated to 98 degrees, revealing a highly hydrophobic surface where the liquid formed pronounced This observation aligns with findings reported by Nawae *et al*., (2021) who similarly noted that an increase in the flow rate resulted in a corresponding increase in the contact angle. In conclusion, the impact of these parameters on the wettability of the Electrospun mat indicates that when the diameter of nanofibers increased, the contact angle also increased under all conditions. This trend can be attributed to the fact that an increase in nanofiber diameter leads to an increase in surface roughness (Borhani *et al*., 2008; Zhou & Wu *et al*., 2015; Zulkefle *et al*., 2020).

3.5 electro spun nanofiber characterization:

To determine the functional groups contained in chemical compositions, FTIR spectroscopy was used as a trustworthy approach. This approach was used to analyze the functional groups in pure PU in comparison to the functional groups identified in the chemical structure of the PU/acetic acid nanofiber sample.

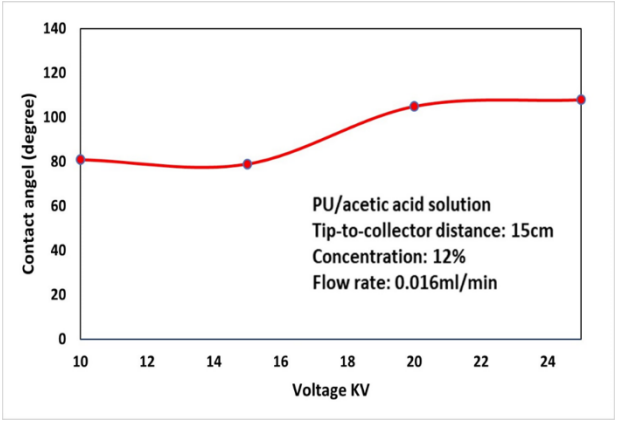

Figure 10: Variation of the contact angle of the water droplet on electrospun polyurethane nanofiber mat with the high voltage.

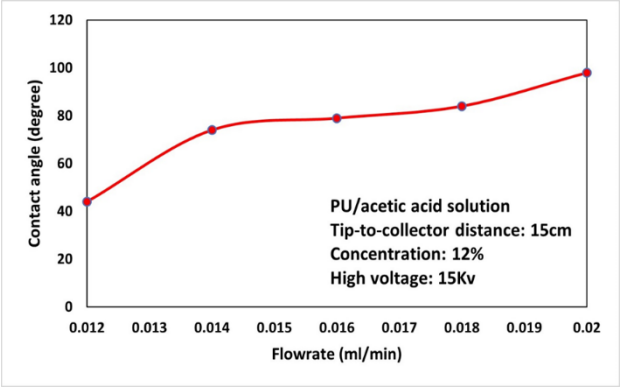

Figure 11: Variation of the contact angle of the water droplet on Electros pun polyurethane nanofiber mat with the solution flow rate.

Figure 12 shows the FTIR spectra of PU and PU/acetic acid that were obtained. In the pure polyurethane spectrum, several distinct peaks are evident. 3302.13 cm^{-1}. This peak is typically associated with the stretching vibration of N-H bonds in urethane groups (NHCO) (Mohammadi *et al*., 2015). Peaks at 2920.23 cm^{-1} and 2850.79 cm^{-1} signify the symmetric and asymmetric stretching vibrations of aliphatic carbon-hydrogen (C-H) bonds, often associated with methyl or methylene groups. Another discernible peak occurs at 2792.93 cm^{-1}, corresponding to the C-H stretching vibration. The peak at 1685.79 cm^-1 is attributed to the carbonyl (C=O) stretching vibration within the urethane groups present in the polyurethane structure. Furthermore, the peak at 1639.49 cm^{-1} can be linked to C=C stretching (Nandiyanto *et al*., 2019). The peak observed at 1523.76 cm^{-1} correspond to nitrogen-hydrogen (N-H) bending vibrations within urethane moieties (Asefnejad *et al*., 2011; Mohammadi *et al*., 2015),

while those at 1446.61 cm^{-1} and 1365.60 cm^{-1} correspond to methylene CH2 and methyl CH3 of saturated aliphatic groups, respectively (Mohammadi *et al*., 2015; Nandiyanto *et al*., 2019). Peaks at 1315.45 cm^{-1} and 1199.72 cm^{-1} are indicative of urethane-related vibrations, particularly involving C-N stretching vibrations. The peak at 1087.85 cm^{-1} might indicate C-O-C stretching within the urethane linkage. At 979.84 cm^{-1}, the peak corresponds to a silicate ion, commonly found among inorganic ions. The peak at 898.83 cm^{-1} suggests bending vibrations of aromatic C-H bonds. Additionally, the peaks at 806.25 cm^{-1} and 779.24 cm^{-1} might be associated with CH bend-out-of-plane vibrations. Finally, the peak at 609.51 cm^{-1} likely corresponds to bending vibrations of alkyne C-H bonds (Nandiyanto *et al*., 2019).

Regarding the polyurethane/acetic acid nanofibers, the

spectra exhibit both similarities to those of pure polyurethane and distinctive features. Specifically, the presence of two peaks at 1712.79 cm^{-1}, indicative of carboxylic acid functionalities, and a peak at 1689.64 cm^{-1}, signifying a conjugated ketone characteristic of the carbonyl compound C=O found in acetic acid, are noteworthy findings (Nandiyanto *et al*., 2019). These observations suggest the enduring presence of residual acetic acid on the nanofiber surface, attributed to the fabrication process. Moreover, a novel peak at 748.38 cm^{-1} emerges, corresponding to methylene (CH2) stretching vibrations, which were notably absent in the pure polyurethane spectra.

When comparing the spectra of pure polyurethane and polyurethane/acetic acid nanofibers, it is evident that the nanofiber spectrum contains peaks associated with acetic acid residues, indicating the retention of some solvent molecules during the nanofiber formation. However, aside from these acetic acid-related peaks, the majority of peaks in the nanofiber spectrum remain consistent with those of pure polyurethane. This guarantees that the overall chemical structure of the polyurethane matrix appears to remain relatively unchanged during the nanofiber formation process, with only minor alterations due to the incorporation of residual acetic acid.

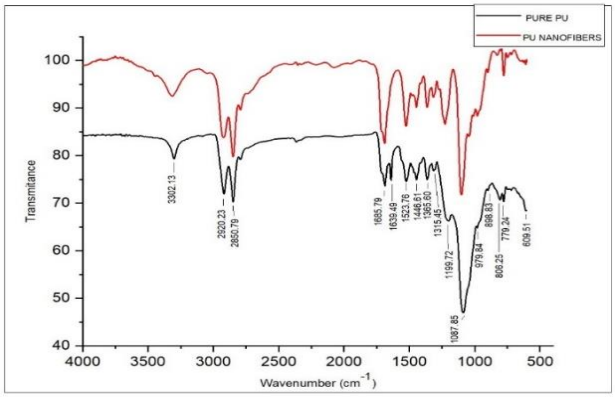

Figure 12: Fourier transforms infrared spectroscopy of pure PU and Electrospun PU.

The crystallographic nature of the PU was determined using X-ray diffraction patterns. Figure 13 illustrates the XRD patterns of the polyurethane nanofiber mat. Notably, there is a broad peak around 2θ = 20° in the sample. This peak corresponds to the distinctive diffraction pattern of the polyurethane polymer. The broadness of this peak is due to the amorphous nature of polyurethane. This diffraction peak appears at an angle of approximately 20°, which closely aligns with observations in other polyurethane material studies (Diani & Gall *et al*., 2006; Sabitha M & Rajiv *et al*., 2015; Hoseini & Nikje *et al*., 2018; Liu *et al*., 2018) . Conversely, the presence of discernible peaks at 2θ = 42.0620° and 48.9590° reveals the existence of crystalline phases within the sample.

These peaks align with the (0 2 5) and (0 2 8) miller indices, corresponding precisely to the crystallographic planes of aluminum oxide hydrate by the JCPDS reference code 98-000-0959. These findings underscore the coexistence of amorphous polyurethane nanofibers and crystalline aluminum oxide hydrate on the substrate. This observation implies that the polyurethane mat was contaminated with traces of aluminum molecules that were stuck on the mat.

Field Emission Scanning Electron Microscopy with Energy Dispersive X-ray Spectroscopy (FESEM-EDX) was utilized for elemental analysis and identification of the composition of Electrospun PU mat, yielding results shown in Figure 14 (a and b). The analysis indicated that the primary elements in the PU nanofiber sample were carbon (C), oxygen (O), and aluminum (Al). This composition aligns with expectations due to the polymeric nature of PU and the substrate. Quantitatively, the composition was approximately 80.35% carbon (C), 19.33% oxygen (O), and 0.32% aluminum (Al) by weight. These percentages highlight carbon and oxygen as dominant, consistent with typical polyurethane composition and these findings are line up with other studies (Nirmala *et al*., 2011; Amina *et al*., 2012). The presence of aluminum, albeit in a minor amount, is attributed to the aluminum foil substrate used for nanofiber deposition.

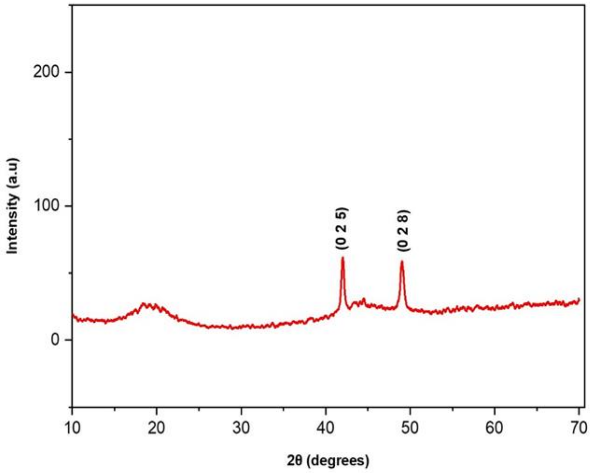

Figure 13 :X-ray diffraction spectra of PU nanofibers.

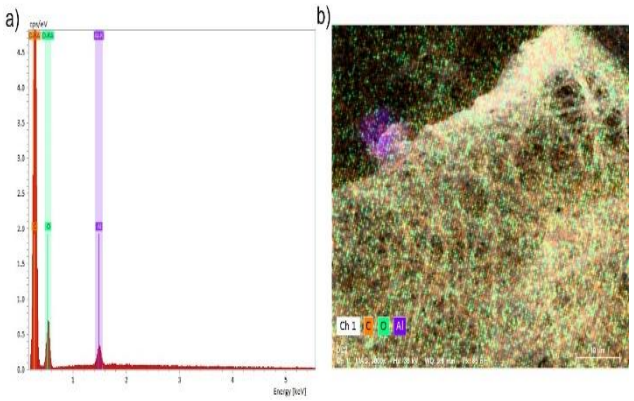

Figure 14: depicts the FESEM-EDX images as follows: (a) displays the peaks associated with the elements found in the sample, while (b) illustrates the layered EDX mapping where each element is represented by a distinct color.

CONCLUSION

Throughout this study, a solution was obtained by dissolving polyurethane polymer in acetic acid and was Electrospun using an electrospinning system. It was concluded that solution concentration, solution flow rate as well as the applied high voltage play a vital role in the adjustment of the morphology and the wettability of the Electrospun nanofiber mat. The study revealed significant impacts on nanofiber morphology and wettability when altering these parameters. Specifically, changing the concentration from 8% to 12% resulted in an increase in nanofiber diameter from 0.326µm to 0.380µm and an increase in the water contact angle from 39° to 79°. Similarly, increasing the flow rate from 0.012ml/min to 0.020ml/min led to the diameter increase from 0.351µm to 0.456µm and an increase in the contact angle from 43° to 98°. Meanwhile, adjusting the voltage from 10kV to 25kV resulted in fluctuations in nanofiber diameter within the range of 0.380µm to 0.497µm. The optimal 12% PU solution concentration was found to eliminate bead formation and ensure uniformity in nanofiber morphology. In addition to these findings, the research also delved into the characterization of the Electrospun PU nanofibers. The FTIR analysis confirmed that the chemical structure of polyurethane did not significantly change when transformed into nanofibers.

Moreover, X-ray diffraction patterns confirmed the amorphous nature of polyurethane while indicating the presence of crystalline phases, notably aluminum oxide hydrate contamination.

REFERENCES:

Akduman, C., & Kumbasar, E. P. A. (2017). Electrospun Polyurethane Nanofibers. *Aspects of Polyurethanes*. https://doi.org/10.5772/intechopen.69937

Amina, M., Al-Youssef, H. M., Amna, T., Hassan, S., El-Shafae, A. M., Kim, H. Y., & Khil, M.-S. (2012). Poly(urethane)/<I>G. Mollis</I> Composite Nanofibers for Biomedical Applications. *Journal of Nanoengineering and Nanomanufacturing*, *2*(1), 85–90. https://doi.org/10.1166/jnan.2012.1056

Asefnejad, A., Khorasani, M. T., Behnamghader, A., Farsadzadeh, B., & Bonakdar, S. (2011). Manufacturing of biodegradable polyurethane scaffolds based on polycaprolactone using a phase separation method: physical properties and in vitro assay. *International Journal of Nanomedicine*, *6*(October), 2375–2384. https://doi.org/10.2147/ijn.s15586

Baji, A., Mai, Y. W., Wong, S. C., Abtahi, M., & Chen, P. (2010). Electrospinning of polymer nanofibers: Effects on oriented morphology, structures and tensile properties. *Composites Science and Technology*, *70*(5), 703–718. https://doi.org/10.1016/j.compscitech.2010.01.010

Banuškevičiute, A., Adomavičiute, E., Milašius, R., & Stanys, S. (2011). Formation of thermoplastic polyurethane (TPU) nano/micro fibers by electrospinning process using electrode with tines. *Medziagotyra*, *17*(3), 287–292. https://doi.org/10.5755/j01.ms.17.3.595

Barhoum, A., Pal, K., Rahier, H., Uludag, H., Kim, I. S., & Bechelany, M. (2019). Nanofibers as new-generation materials: From spinning and nano-spinning fabrication techniques to emerging applications. *Applied Materials Today*, *17*, 1–35. https://doi.org/10.1016/j.apmt.2019.06.015

Beachley, V., & Wen, X. (2010). Polymer nanofibrous structures: Fabrication, biofunctionalization, and cell interactions. *Progress in Polymer Science (Oxford)*, *35*(7), 868–892. https://doi.org/10.1016/j.progpolymsci.2010.03.003

Bhardwaj, N., & Kundu, S. C. (2010). Electrospinning: A fascinating fiber fabrication technique. *Biotechnology Advances*, *28*(3), 325–347. https://doi.org/10.1016/j.biotechadv.2010.01.004

Borhani, S., Hosseini, S. A., Etemad, S. G., & Militký, J. (2008). Structural characteristics and selected properties of polyacrylonitrile nanofiber mats. *Journal of Applied Polymer Science*, *108*(5), 2994-3000.

Chen, H. W., & Lin, M. F. (2020). Characterization, biocompatibility, and optimization of electrospun SF/PCL/CS composite nanofibers. *Polymers*, *12*(7). https://doi.org/10.3390/polym12071439

Choi, H. J., Kim, S. B., Kim, S. H., & Lee, M. H. (2014). Preparation of electrospun polyurethane filter media and their collection mechanisms for ultrafine particles. *Journal of the Air and Waste Management Association*, *64*(3), 322–329. https://doi.org/10.1080/10962247.2013.858652

Colmenares-Roldán, G. J., Quintero-Martínez, Y., Agudelo-Gómez, L. M., Rodríguez- Vinasco, L. F., & Hoyos-Palacio, L. M. (2017). Influence of the molecular weight of polymer, solvents and operational condition in the electrospinning of polycaprolactone. *Revista Facultad de Ingenieria*, *2017*(84), 35–45. https://doi.org/10.17533/udea.redin.n84a05

Demir, M. M., Yilgor, I., Yilgor, E., & Erman, B. (2002). Electrospinning of polyurethane ®bers M.M. *Polymer*, *43*, 3303–3309.

Diani, J., & Gall, K. (2006). Finite Strain 3D Thermoviscoelastic Constitutive Model. *Society*, 1–10. https://doi.org/10.1002/pen

Eatemadi, A., Daraee, H., Zarghami, N., Yar, H. M., & Akbarzadeh, A. (2016). Nanofiber: Synthesis and biomedical applications. *Artificial Cells, Nanomedicine and Biotechnology*, *44*(1), 111–121. https://doi.org/10.3109/21691401.2014.922568

Emad Abdoluosefi, H., & Honarasa, G. (2017). Fabrication of polyurethane and thermoplastic polyurethane nanofiber by controlling the electrospinning parameters. *Materials Research Express*, *4*(10). https://doi.org/10.1088/2053-1591/aa9191

Firoozi, S., Amani, A., Derakhshan, M. A., & Ghanbari, H. (2016). Artificial Neural Networks modeling of electrospun polyurethane nanofibers from chloroform/methanol solution. *Journal of Nano Research*, *41*, 18–30. https://doi.org/10.4028/www.scientific.net/JNanoR.41.18

Fong, H., Chun, I., & Reneker, D. H. (1999). Beaded nanofibers formed during electrospinning. *Polymer*, *40*(16), 4585-4592

Gao, C., Zhang, L., Wang, J., Jin, M., Tang, Q., Chen, Z., Cheng, Y., Yang, R., & Zhao, G. (2021). Electrospun nanofibers promote wound healing: theories, techniques, and perspectives. *Journal of Materials Chemistry B*, *9*(14), 3106–3130. https://doi.org/10.1039/d1tb00067e

Greiner, A., & Wendorff, J. H. (2007). Electrospinning: A fascinating method for the preparation of ultrathin fibers. *Angewandte Chemie - International Edition*, *46*(30), 5670–5703. https://doi.org/10.1002/anie.200604646

Hale Karakaş. (2012). Electrospinning of nanofibers and their applications. *MDT "Electrospinning," 3*, 1–35. http://www.pdfdrive.net/electrospinning-of-nanofibers-and-their-applications-e34353447.html

Hoseini, Z., & Nikje, M. M. A. (2018). Synthesis and characterization of a novel thermally stable water dispersible polyurethane and its magnetic nanocomposites. *Iranian Polymer Journal (English Edition)*, *27*(10), 733–743. https://doi.org/10.1007/s13726-018-0650-5

Hu, J., Liu, C., & Lin, C. (2021). *李莹-Synthesis, characterization and electrospinning of new thermoplastic.pdf*.

Karakaş, H., Jahangiri, S., Saraç, A. S., Karakaş, H., Jahangiri, S., Structure, A. S. S., Parameter, P., Karakaş, H., Jahangiri, S., & Saraç, A. S. (2018). *Electrospun Nanofibers To cite this version : HAL Id : hal-01894397 Structure and Process Parameter Relations of Electrospun Nanofibers*.

Karakaş, H., Saraç, A., Polat, T., & Budak, E. (2013). Polyurethane Nanofibers Obtained By Electrospinning Process. *International Journal of Biological, Biomolecular, Agricultural, Food and Biotechnology Engineering*, *7*(3), 177–180. http://waset.org/journals/waset/v75/v75-111.pdf

Khan, Z., Kafiah, F., Zahid Shafi, H., Nufaiei, F., Ahmed Furquan, S., & Matin, A. (2015). Morphology, Mechanical Properties and Surface Characteristics of Electrospun Polyacrylonitrile (PAN) Nanofiber Mats. *International Journal of Advanced Engineering and Nano Technology*, *February*, 2347–6389.

Kiliç, E., Yakar, A., & Pekel Bayramgil, N. (2018). Preparation

of electrospun polyurethane nanofiber mats for the release of doxorubicine. *Journal of Materials Science: Materials in Medicine*, *29*(1). https://doi.org/10.1007/s10856-017-6013-5

Li, B., Liu, Y., Wei, S., Huang, Y., Yang, S., Xue, Y., Xuan, H., & Yuan, H. (2020). A solvent system involved fabricating electrospun polyurethane nanofibers for biomedical applications. *Polymers*, *12*(12), 1–12. https://doi.org/10.3390/polym12123038

Li, Z., Wang, C., & Zhenyu LI. (2016). *Zhenyu Li · Ce Wang One-Dimensional Nanostructures Electrospinning Technique and Unique Nanofibers* (Issue November). https://doi.org/10.1007/978-3-642-36427-3

Liu, M., Liu, T., Chen, X., Yang, J., Deng, J., He, W., Zhang, X., Lei, Q., Hu, X., Luo, G., & Wu, J. (2018). Nano-silver-incorporated biomimetic polydopamine coating on a thermoplastic polyurethane porous nanocomposite as an efficient antibacterial wound dressing. *Journal of Nanobiotechnology*, *16*(1), 1–19. https://doi.org/10.1186/s12951-018-0416-4

Matabola, K. P., de Vries, A. R., Luyt, A. S., & Kumar, R. (2011). Studies on single polymer composites of poly(methyl methacrylate) reinforced with electrospun nanofibers with a focus on their dynamic mechanical properties. *Express Polymer Letters*, *5*(7), 635–642. https://doi.org/10.3144/expresspolymlett.2011.61

Mohammadi, A., Barikani, M., & Barmar, M. (2015). Synthesis and investigation of thermal and mechanical properties of in situ prepared biocompatible Fe3O4/polyurethane elastomer nanocomposites. *Polymer Bulletin*, *72*(2), 219–234. https://doi.org/10.1007/s00289-014-1268-1

Nandiyanto, A. B. D., Oktiani, R., & Ragadhita, R. (2019). How to read and interpret ftir spectroscope of organic material. *Indonesian Journal of Science and Technology*, *4*(1), 97–118. https://doi.org/10.17509/ijost.v4i1.15806

Nawae, S., Tohluebaji, N., Putson, C., Muensit, N., & Yuennan, J. (2021). Effect of flow rate on the fabrication of P(VDF-HFP) nanofibers. *Journal of Physics: Conference Series*, *1719*(1). https://doi.org/10.1088/1742-6596/1719/1/012070

Nirmala, R., Nam, K. T., Navamathavan, R., Park, S. J., & Kim, H. Y. (2011). Hydroxyapatite Mineralization on the Calcium Chloride Blended Polyurethane Nanofiber via Biomimetic Method. *Nanoscale Research Letters*, *6*(1), 1–8. https://doi.org/10.1007/s11671-010-9737-4

Nitanan, T., Opanasopit, P., Akkaramongkolporn, P., Rojanarata, T., Ngawhirunpat, T., & Supaphol, P. (2012). Effects of processing parameters on morphology of electrospun polystyrene nanofibers. *Korean Journal of Chemical Engineering*, *29*(2), 173–181. https://doi.org/10.1007/s11814-011-0167-5

Öteyaka, M. Ö., Aybar, K., & Öteyaka, H. C. (2022). A comparative study of the effect of polyurethane nanofiber and powders filler on the mechanical properties of carbon fiber and glass fiber composites. *Pamukkale University Journal of Engineering Sciences*, *28*(1), 51–57. https://doi.org/10.5505/pajes.2021.73659

Panwiriyarat, W. (2013). Preparation and properties of bio-based polyurethane made from natural rubber and poly (Ɛ-caprolactone) (Doctoral dissertation, Prince of Songkla University).

Rabbi, A., Nasouri, K., Bahrambeygi, H., Shoushtari, A. M., & Babaei, M. R. (2012). RSM and ANN approaches for modeling and optimizing of electrospun polyurethane nanofibers morphology. *Fibers and Polymers*, *13*(8), 1007–1014. https://doi.org/10.1007/s12221-012-1007-x

Sharma, J., Lizu, M., Stewart, M., Zygula, K., Lu, Y., Chauhan, R., Yan, X., Guo, Z., Wujcik, E. K., & Wei, S. (2015). Multifunctional nanofibers towards active biomedical therapeutics. In *Polymers* (Vol. 7, Issue 2). https://doi.org/10.3390/polym7020186

Sorlier, P. (2007). Electrospinning and nanofibers. In *Polymers: Last achievements and prospects, in honour of Professor Jérôme*. http://hdl.handle.net/2268/11512

Sabitha, M., & Rajiv, S. (2015). Preparation and characterization of ampicillin-incorporated electrospun polyurethane scaffolds for wound healing and infection control. *Polymer Engineering & Science*, *55*(3), 541-548.

Ungur, G., & Hrůza, J. (2017). Modified polyurethane nanofibers as antibacterial filters for air and water purification. *RSC Advances*, *7*(78), 49177–49187. https://doi.org/10.1039/c7ra06317b

Wang, N., Burugapalli, K., Song, W., Halls, J., Moussy, F., Zheng, Y., Ma, Y., Wu, Z., & Li, K. (2013). Tailored fibro-porous structure of electrospun polyurethane membranes, their size-dependent properties and trans-membrane glucose diffusion. *Journal of Membrane Science*, *427*(January), 207–217. https://doi.org/10.1016/j.memsci.2012.09.052

Williams, G. R., Raimi-Abraham, B. T., & Luo, C. J. (2018). Electrospinning fundamentals. *Nanofibres in Drug Delivery*, 24–59. https://doi.org/10.2307/j.ctv550dd1.6

Yang, Z., Peng, H., Wang, W., & Liu, T. (2010). Crystallization behavior of poly(ε-caprolactone)/layered double hydroxide nanocomposites. *Journal of Applied Polymer Science*, *116*(5), 2658–2667. https://doi.org/10.1002/app

Yi, B., Zhao, Y., Tian, E., Li, J., & Ren, Y. (2019). High-performance polyimide nanofiber membranes prepared by electrospinning. *High Performance Polymers*, *31*(4), 438–448. https://doi.org/10.1177/0954008318781703

Zhou, Z., & Wu, X. F. (2015). Electrospinning superhydrophobic-superoleophilic fibrous PVDF membranes for high-efficiency water-oil separation. *Materials Letters*, *160*, 423–427. https://doi.org/10.1016/j.matlet.2015.08.003

Zulkefle, M. A., Abid, S. A. U. S. M., Rahman, R. A., Zulkifli, Z., & Herman, S. H. (2020). Polyvinylpyrrolidone matrix concentration effects on the physical properties of TiO2nanofibers prepared using electrospinning method. *AIP Conference Proceedings*, *2306*. https://doi.org/10.1063/5.0032775

Zuo, W., Zhu, M., Yang, W., Yu, H., Chen, Y., & Zhang, Y. (2005). Experimental study on relationship between jet instability and formation of beaded fibers during electrospinning. *Polymer Engineering and Science*, *45*(5), 704–709. https://doi.org/10.1002/pen.20304

Zhuo, H., Hu, J., & Chen, S. (2008). Electrospun polyurethane nanofibres having shape memory effect. *Materials Letters*, *62*(14), 2074-2076.